Materials Research Proceedings 28 (2023) 1621-1630 https://doi.org/10.21741/9781644902479-175

Physics-informed machine learning in the determination of effective thermomechanical properties

SOYARSLAN Celal[1,2,a *] and PRADAS Marc[3,b]

[1]Chair of Nonlinear Solid Mechanics, University of Twente, The Netherlands

[2]Fraunhofer Innovation Platform, University of Twente, The Netherlands

[3]School of Mathematics and Statistics, The Open University, United Kingdom

[a]c.soyarslan@utwente.nl,[b] bmarc.pradas@open.ac.uk

Keywords: PINNs, Computational Homogenization, Thermomechanics, Effective Properties

Abstract. We determine the effective (macroscopic) thermoelastic properties of two-phase composites computationally. To this end, we use a physics-informed neural network (PINN)-mediated first-order two-scale periodic asymptotic homogenization framework. A diffuse interface formulation is used to remedy the lack of differentiability of property tensors at phase interfaces. Considering the reliance on the standard integral solution for the property tensors on only the gradient of the corresponding solutions, the emerging unit cell problems are solved up to a constant. In view of this and the exact imposition of the periodic boundary conditions, it is merely the corresponding differential equation that contributes to minimizing the loss. This way, the requirement of scaling individual loss contributions of different kinds is abolished. The developed framework is applied to a planar thermoelastic composite with a hexagonal unit cell with a circular inclusion by which we show that PINNs work successfully in the solution of the corresponding thermomechanical cell problems and, hence, the determination of corresponding effective properties.

Introduction

Accurate prediction of the effective (macroscopic) material properties is crucial for the high-fidelity simulation of the deformation processes of heterogeneous media. Although there exist analytically derived bounds, e.g., (arithmetic) Voigt and the (harmonic) Reuss averages;
and effective-medium theories, e.g., the Maxwell, self-consistent, and differential effective-medium approximations, these fall short of providing accurate predictions for materials systems, including high property contrast and varying phase volume fractions [1]. This is due to the limited microstructural descriptors considered in their formulation, e.g., the phase volume fraction and shape. As a remedy, full-field computational micro-macro transfer techniques, e.g., finite element method-based computational homogenization schemes, have been proposed [2-5]. This requires solving the boundary value problem, in this context also referred to as the *cell problem*, over the discretized periodic unit cell, or, in general, a representative volume element (RVE).

Since the founding work of Lagaris *et al*., [6] deep neural networks (DNNs) have emerged as an alternative method to solve partial differential equations (PDEs). Physics-informed neural networks (PINNs) use the universal approximation property [7-9] of DNNs in approximating the solution of PDEs in physical problems[10]. This is accomplished through an optimization procedure in which the DNN hyper-parameters are found by minimizing loss functions.
Whereas the classical machine learning approaches identify the corresponding error in terms of distance to a dataset, it is the residual norm of the governing differential equation and associated initial and boundary conditions (BCs) which forms the loss function in PINNs [6, 11-13]. As opposed to standard discretization techniques, e.g., the finite element method (FEM), which

requires domain discretization and construction of a weak form, PINNs allow solving the PDE in its strong form and in a meshless manner providing a differentiable solution which proves helpful in subsequent calculations[6]. For an extensive survey regarding the state of the art of PINNs, the reader is referred to [14].

This work considers the determination of the effective thermomechanical properties of periodic two-phase composites. This is accomplished by two-scale asymptotic and computational homogenization. Unlike many references that conventionally use FEM in the solution of the cell problem, see, e.g., [2-5], we use PINNs by considering that the micro- (constituent-level) \MP{scale} is described by Duhamel-Neumann and Fourier laws. Solving the unit cell problems up to a constant and an exact imposition of the periodic boundary conditions eliminates loss contributions from the boundary conditions of different kinds. It should be noted that the property tensor computations rely on the integrals of the gradient of the corresponding solutions.
DeepXDE is used as the scientific ML and physics-informed library[10]. A 2D periodic hexagonal unit cell with a central circular inclusion is selected as an application problem. Our work shows that PINNs successfully solve the cell problem, i.e., the local thermomechanical boundary value problem, and determine corresponding effective properties. For an extended treatment of the framework in generic elliptic PDEs, with $n-$dimensional applications including phase contrast and interface sharpness effects on the solution accuracy, see [15].

Planar Thermoelasticity

We consider planar thermoelasticity in which the relation between mechanical and thermal fields is constructed through the following Duhamel-Neumann law [16,17] for *i,j,k,l* = 1,2

$$\sigma_{ij} = \mathrm{C}_{ijkl}\epsilon_{ij} - \beta_{ij}\Theta \tag{1}$$

$$\beta_{ij} = \mathrm{C}_{ijkl}\alpha_{kl} \tag{2}$$

Here, C_{ijkl}, β_{ij}, and α_{kl} denote components of the fourth-order planar elasticity tensor C, and planar second-order thermal expansion tensors β and κ, respectively. The temperature field is denoted by Θ whereas σ represents the stress tensor. Letting x denote the position vector, the components of the strain tensor ϵ are computed from the displacement field u with

$$\epsilon_{ij} = \frac{1}{2}\left[\frac{\partial u_i}{\partial x_j} + \frac{\partial u_j}{\partial x_i}\right] \tag{3}$$

Letting κ denote the second-order thermal conductivity tensor; it is assumed that Fourier law relates the heat flow vector to the temperature with

$$q_i = -\kappa_{ij}\frac{\partial \Theta}{\partial x_j} \tag{4}$$

In view of Eq. 1 and 4, and letting b and f denote the internal body force and heat source density, respectively, the linear momentum balance and the stationary heat balance equations respectively read

$$\frac{\partial \sigma_{ij}}{\partial x_j} = b_i \qquad and \qquad \frac{\partial q_i}{\partial x_i} = f \tag{5}$$

Considering planar thermoelastic isotropy, we have

$$C_{ijkl} = \lambda\delta_{ij}\delta_{kl} + \mu\left[\delta_{il}\delta_{jk} + \delta_{ik}\delta_{jl}\right], \qquad \beta_{ij} = \beta\delta_{ij}, \qquad and \qquad \kappa_{ij} = \kappa\delta_{ij} \tag{6}$$

for *i, j, k, l* = 1, 2. Here, λ and μ represent planar Lamé constants, whereas β and κ denote isotropic thermal expansion and heat conduction coefficients. In matrix notation, the isotropic property tensors C, β, and κ whose indicial representations are given in Eq. 6, correspond to the following 3 x 3, 2 x 2, and 2 x 2 matrices, respectively

$$[C] = \begin{bmatrix} \lambda + 2\mu & \lambda & 0 \\ \lambda & \lambda + 2\mu & 0 \\ 0 & 0 & \mu \end{bmatrix}, \quad [\beta] = \begin{bmatrix} \beta & 0 \\ 0 & \beta \end{bmatrix}, \quad [\kappa] = \begin{bmatrix} \kappa & 0 \\ 0 & \kappa \end{bmatrix} \tag{7}$$

First-Order Asymptotic Homogenization

We are interested in material systems of two periodically distributed phases showing linear physical properties. For such systems, a repeating material domain *v*, which is also referred to as a unit cell, encapsulates all material characteristics. Henceforth, let *x* denote the cell-scale (microscale) position and capture fast field variations. It is linked to the macroscale position ${}^{M}x$ which captures fields slow variations, with $x = {}^{M}x/\epsilon$, where $0 < \epsilon << 1$ scale separation parameter. Following [17], we apply a two-scale asymptotic expansion of the *nondimensional* thermoelastic problem-solution in terms of the displacement and temperature fields $u^{\epsilon}({}^{M}x)$ and $\Theta^{\epsilon}({}^{M}\boldsymbol{x})$ results in the following representation

$$u^{\epsilon}\left({}^{M}x\right) = u^{(0)}\left({}^{M}x, x\right) + \epsilon u^{(1)}\left({}^{M}x, x\right) + \epsilon^2 u^{(2)}\left({}^{M}x, x\right) + O(\epsilon^3) \tag{8}$$

$$\Theta^{\epsilon}\left({}^{M}x\right) = \Theta^{(0)}\left({}^{M}x, x\right) + \epsilon u\Theta^{(1)}\left({}^{M}x, x\right) + \epsilon^2 u\Theta^{(2)}\left({}^{M}x, x\right) + O(\epsilon^3) \tag{9}$$

Here, $u^{(i)}$ and $\Theta^{(i)}$ are *v* periodic functions in *x*. Using Eq. 1 and 4 to derive the expansions for the stress tensor and heat flux vector, σ^{ϵ} and q^{ϵ}, substituting the expansions in Eq. 5 and comparing coefficients of powers in ϵ and applying separation of variables, we reach the following macroscopic property tensors $C^{\star}$, $\beta^{\star}$, and $\kappa^{\star}$, respectively

$$C^{*}_{ijkl} = \frac{1}{|v|}\int_{v} \left[C_{ijkl} + C_{ijmn}\frac{\partial U^{kl}_{m}(x)}{\partial x_n}\right] dV \tag{10}$$

$$\beta^{*}_{ij} = \frac{1}{|v|}\int_{v} \left[\beta_{ij} - C_{ijmn}\frac{\partial L_m(x)}{\partial x_n}\right] dV \tag{11}$$

$$\kappa^{*}_{ij} = \frac{1}{|v|}\int_{v} \left[\kappa_{ij} - \kappa_{nj}\frac{\partial M^{i}(x)}{\partial x_n}\right] dV \tag{12}$$

In Eq. 10, 11 and 12, ${U^{kl}}_{m}$, L_m and M^i for *m, k, l, i* = 1, 2 correspond to v - periodic corrector functions which constitute the solutions of the following cell-problems, respectively

$$\frac{\partial}{\partial x_j}\left[C_{ijkl}\frac{\partial U^{mn}_{k}(x)}{\partial x_l}\right] = -\frac{\partial C_{ijmn}(x)}{\partial x_j} \tag{13}$$

$$\frac{\partial}{\partial x_j}\left[C_{ijkl}\frac{\partial L_k(x)}{\partial x_l}\right] = \frac{\partial \beta_{ij}(x)}{\partial x_j} \tag{14}$$

$$\frac{\partial}{\partial x_j}\left[\kappa_{jl}\frac{\partial M^{i}(x)}{\partial x_l}\right] = -\frac{\partial \kappa_{ij}(x)}{\partial x_j} \tag{15}$$

Physics-Informed Neural Networks (PINNs)

In the representation of the corresponding theory, we follow the works by Lu *et al.* [10] and Haghighat *et al.* [13]. Let $N^L(x;\Theta) : \mathrm{R}^{\dim_{in}} \rightarrow \mathrm{R}^{\dim_{out}}$ represent the surrogate model, an L-layer neural network with L - 1 number of hidden layers, that gives the approximate solution for the unknown u of the differential equation. Let x and y denote the input and output vectors, respectively, and $\Theta := \{W, b\}$ represent the set of trainable network parameters, i.e., the weight matrix W and the bias vector b. $\dim_{in}$ and $\dim_{out}$ denote the network input and output dimensions, respectively. With the input-output relations $z^0 \leftarrow x$ and $y \leftarrow z^L$, the propagation of the input through the layers of a feed-forward network is accomplished with the following sequence of operations

$$z^k = \sigma(W^k z^{k-1} + b^k), \qquad 1 \leq k \leq L-1 \tag{16}$$

$$z^L = W^L z^{L-1} + b^L \tag{17}$$

Here, σ is the nonlinear activation function, and q_k, $z^k \in \mathrm{R}^{q_k}$, $W^k \in \mathrm{R}^{q_k \times q_{k-1}}$ and $b^k \in \mathrm{R}^{q_k}$ denote the number of neurons, the outputs, the weight matrix, and the bias vector of each layer k, espectively.

Fig. 1 depicts a schematic plot of a PINN used in the solution of PDEs for the input x and output $\hat{u}$, as an approximation of the actual solution u. P and B respectively denote the differential and boundary operators and the subscripts P and B associations with the PDE and the boundary operators, respectively. For a given training set (collocation points) T, the loss function $L(\boldsymbol{\theta}; T)$ then comprises a weighted sum (with ω_P and ω_B denoting the loss weights) of the residuals of the PDE and the boundary terms which are denoted by $L_P(\boldsymbol{\theta}; T_P)$) and $L_B(\boldsymbol{\theta}; T_B)$), respectively, to give

$$L(\theta; T) = \omega_P L_P(\theta; T_P) + \omega_B L_{PB}(\theta; T_B) \tag{18}$$

The neural network minimizes the loss function by varying the network parameters θ by means of a process referred to as training. At the end of the training, a converged parameter set $\boldsymbol{\theta}^\star$ is reached, providing the optimum output.

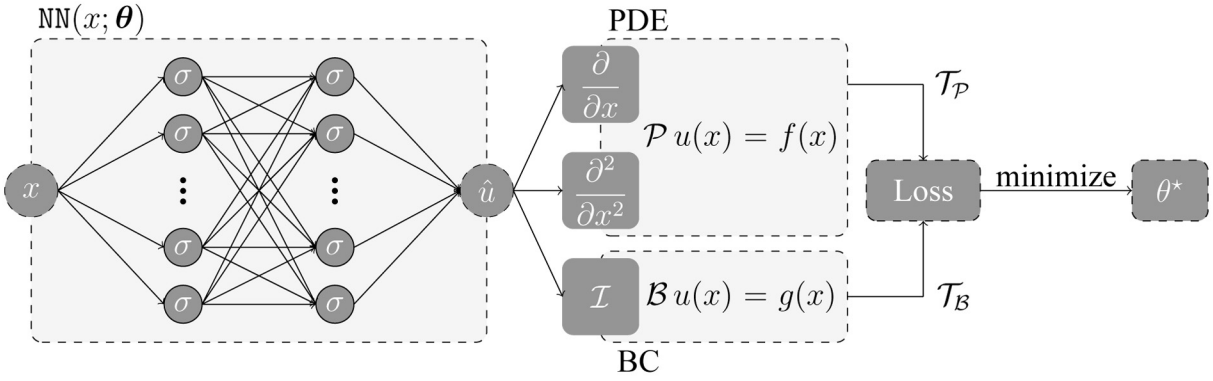

Fig. 1. Schematics of a PINN used in the solution of a PDE with P and B denoting differential and boundary operators, respectively. The image is adapted from [10].

Applications

As an illustrative example, we consider a two-dimensional hexagonal composite domain with a circular inclusion. The selected unit cell corresponds to the Wigner-Seitz cell of the hexagonal Bravais lattice; see Fig. 2. An inclusion volume fraction of $\phi_i = 0.30$ is selected.

Letting $a(x)$ denote a generic isotropic property; the inclusion and matrix properties are denoted as a_i and a_m, respectively. For convenience we consider the values $a_i = \lambda_i = \mu_i = \beta_i = \kappa_i = 2$ and $a_m = \lambda_m = \mu_m = \beta_m = \kappa_m = 1$. This corresponds to a property contrast of 2. The case for phase interchange with $a_i = 1$ and $a_m = 2$ is also investigated.

Considering Eq. 13, 14 and 15, the computation of the source terms requires property derivatives with respect to position. To make this possible, we use a diffuse interface approach given by

$$a(x) = a_m + \frac{a_i - a_m}{2}\left[1 - \tanh\left(\frac{|x|-r}{\xi}\right)\right] \tag{19}$$

where the regularization parameter ξ is chosen to satisfy $L/\xi = 200$. In view of Neumann's principle [18, 19], the macroscopic thermoelastic properties of the material system represented by the periodic composite unit cell given in Fig. 2 possess planar isotropy. Consequently, we can compute the thermoelastic property tensor components through the solutions $U^{kl}{}_m$, L_m and M^i of Eq. 13, 14 and 15 using only one source term in each, which we denote by b^U, b^L and f^M, respectively, and are given in matrix form as

$$[b^U] = \begin{bmatrix} \frac{\partial[\lambda(x)+2\mu(x)]}{\partial x_1} \\ \frac{\partial \lambda(x)}{\partial x_2} \end{bmatrix}, \qquad [b^L] = \begin{bmatrix} \frac{\partial \beta(x)}{\partial x_1} \\ \frac{\partial B(x)}{\partial x_2} \end{bmatrix}, \qquad and \qquad f^M = \frac{\partial \kappa(x)}{\partial x_1} \tag{20}$$

The above problem is implemented into DeepXDE, a scientific ML and physics-informed library [10]. As for the NN hyperparameters, the density and depth of the neural network are selected as 50 and 3, respectively. 25000 collocation points are selected over the problem domain. In optimization studies, a learning rate of 0.01 is used with 30000 epochs. The first 5000 of the 30000 epochs belong to adam optimizer, whereas the remaining 25000 to the L-BFGS optimizer.

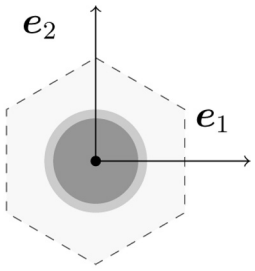

Fig. 2. The selected hexagonal unit cell centered at the origin of the selected Cartesian plane (e_1, e_2). The regular hexagon has an edge length of L and the circular inclusion a radius of r. A diffuse phase interface formulation makes the function differentiable when computing the source terms.

Results and Discussions

Using the PINNs framework, the cell problems dictated by Eq. 13, 14 and 15 are solved for the load cases given in Eq. 20 considering phase properties with $a_i/a_m = 2$ and $a_m/a_i = 2$. Fig. 3 gives the normalized loss function training histories for the PINN solutions. During the iterations, the

first 5000 epochs belonged to the first-order and stochastic adam optimizer. It is observed thatat the latter stages of adam optimization, the loss hardly improves. Reverting to L-BFGS optimizer considerably reduces loss by providing a monotonic convergence.

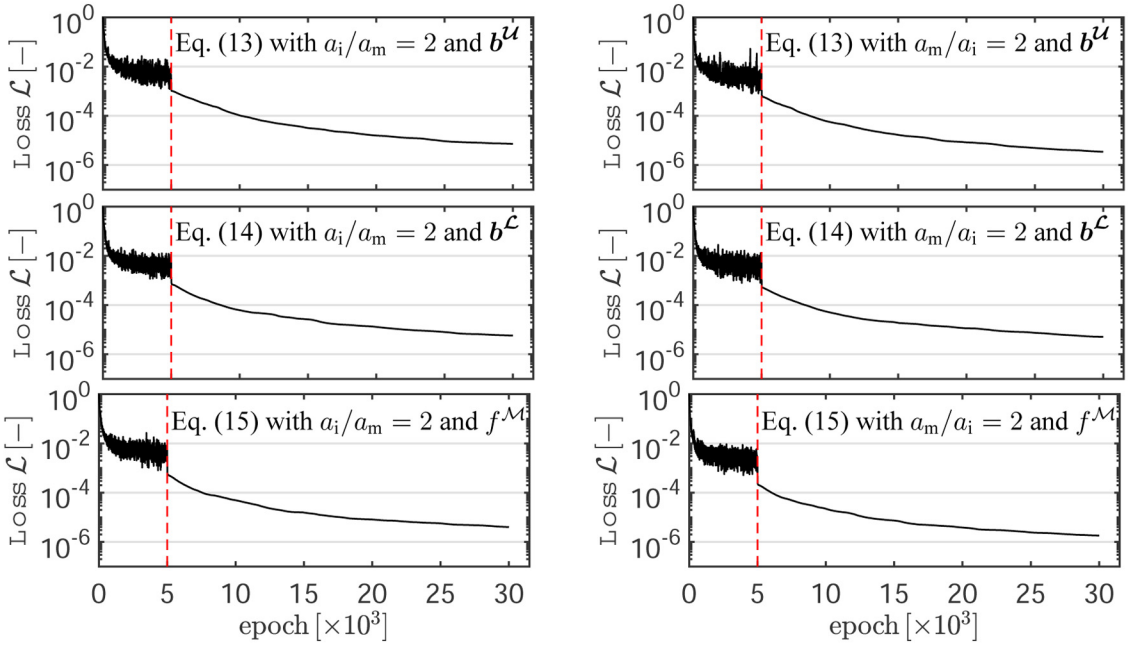

Fig. 3. Training histories of the loss function for the PINN solution of the cell problems given in Eq. 13, 14 and 15. The first 5000 epochs (marked with a red dashed line) belong to adam optimizer, whereas the remaining to L-BFGS. All results are normalized with respect to the initial state.

Resultant contour plots for the property, as well as resultant fields, are given in Figs. 4, 5, and 6. The symmetry and periodicity in the solution fields match that of the composite unit cell. The phase interchange results in the interchange of zones of maximum and minimum in the field distributions.

Computing the integral expressions given in Eq. 10, 11 and 12, we determine the effective property tensors. For $a_i/a_m = 2$ and phase content of $\phi_i = 0.30$, the (arithmetic) Voigt and the (harmonic) Reuss averages yield $a^*_V = 1.300$ and $a^*_R = 1.176$, respectively, which also correspond to upper and lower bounds, respectively.

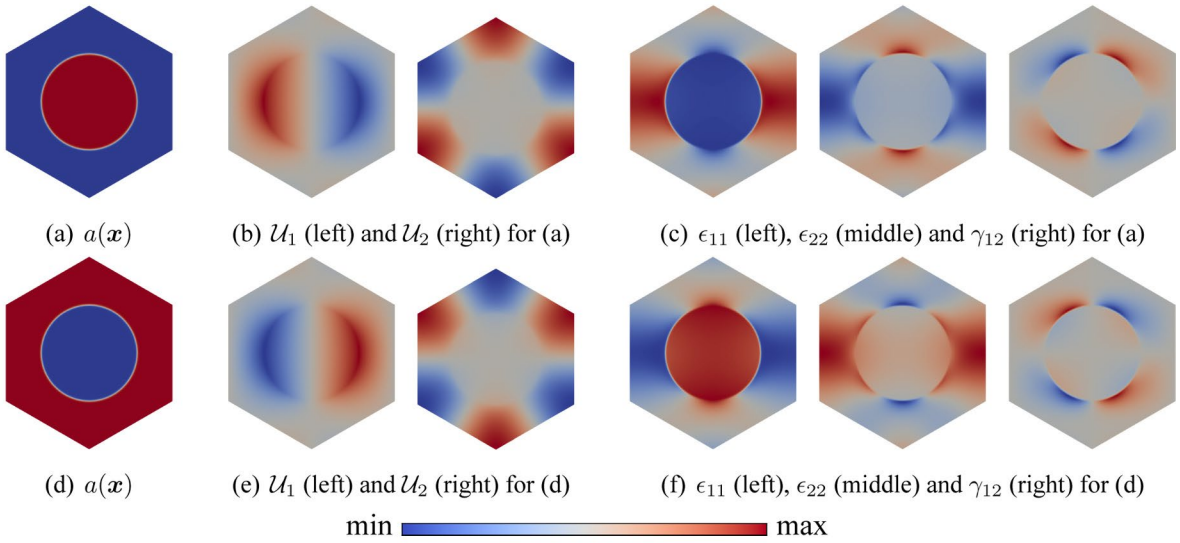

Fig. 4. The contour plots for the solution of Eq. 13 considering the load case b^U given in Eq. 20. The property field a(x) is given for $a_i/a_m = 2$ in (a) and for $a_m/a_i = 2$ in (d). The strain components are computed using the corresponding corrector function U with $\epsilon_{11} = \partial U_1/\partial x_1$, $\epsilon_{22} = \partial U_2/\partial x_2$ and $\gamma_{12} = [\partial U_1/\partial x_2 + \partial U_2/\partial x_1]$.

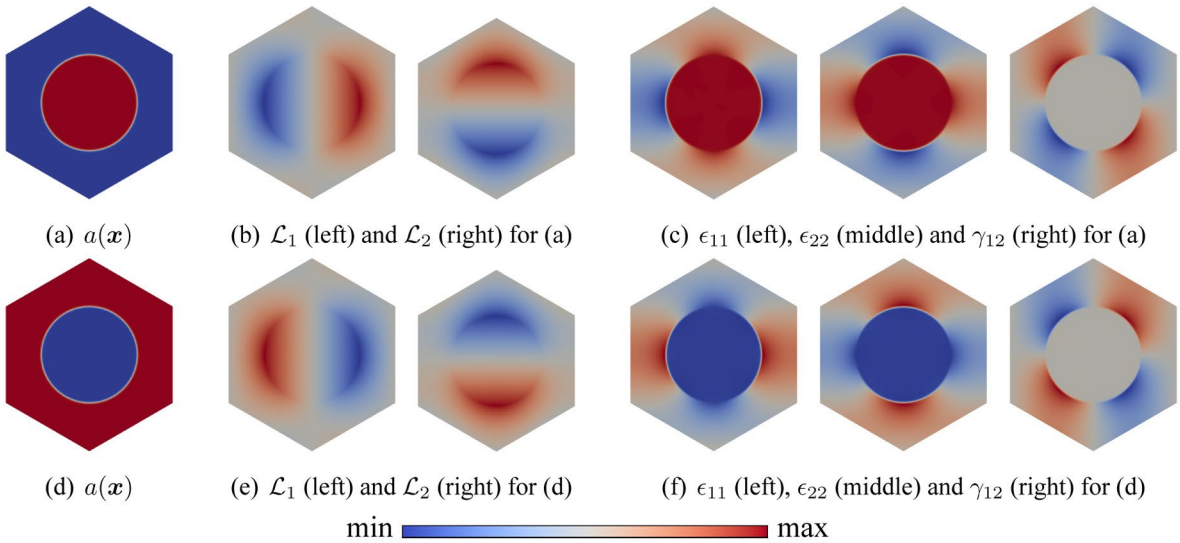

Fig. 5. The contour plots for the solution of Eq. 14 considering the load case b^L given in Eq. 20. The property field a(x) is given for $a_i/a_m = 2$ in (a) and for $a_m/a_i = 2$ in (d). The strain components are computed using the corresponding corrector function L with $\epsilon_{11} = \partial L_1/\partial x_1$, $\epsilon_{22} = \partial L_2/\partial x_2$ and $\gamma_{12} = [\partial L_1/\partial x_2 + \partial L_2/\partial x_1]$.

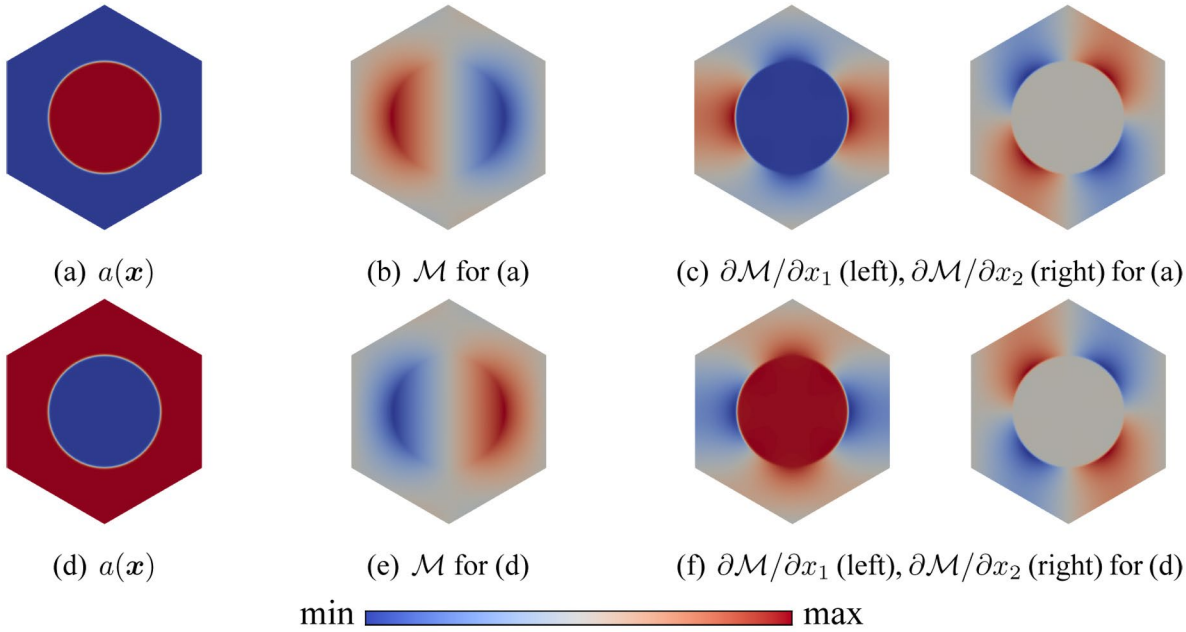

Fig. 6. The contour plots for the solution of Eq. 15 considering the load case $f^{\mathcal{M}}$ given in Eq. 20. The property field a(x) is given for $a_i/a_m = 2$ in (a) and for $a_m/a_i = 2$ in (d).

This is, however, under sharp interface conditions, which is not the case in our PINN computations. In our PINN solution, we have the following matrix representations

$$[C^*] = \begin{bmatrix} 3.621 & 1.207 & 0 \\ 1.207 & 3.621 & 0 \\ 0 & 0 & 1.207 \end{bmatrix}, \quad [\beta^*] = \begin{bmatrix} 1.207 & 0 \\ 0 & 1.207 \end{bmatrix}, \quad [\kappa^*] = \begin{bmatrix} 1.224 & 0 \\ 0 & 1.224 \end{bmatrix}$$

This corresponds to the effective planar Lamé constants of $\lambda^* = \mu^* = 1.207$. Selecting $\lambda = \mu$ and keeping a constant ratio between the λ, μ, and β values of the matrix and the inclusion corresponds to the assumption of an identical thermal expansion coefficient α for the phases. Consequently, one expects to recover $\alpha^* = \alpha_i = \alpha_m = 1/4$ as the effective thermal expansion coefficient for the composite. Our solutions with $\beta^* = \lambda^* = \mu^*$ agree with this statement and confirm our computations. Taking $a_m/a_i = 2$ and phase content of $\phi_i = 0.30$, the (arithmetic) Voigt and the (harmonic) Reuss averages, considering sharp interface conditions, yield $a^*_V = 1.700$ and $a^*_R = 1.538$, respectively. In our PINN solution, we have the following matrix representations

$$[C^*] = \begin{bmatrix} 4.830 & 1.610 & 0 \\ 1.610 & 4.830 & 0 \\ 0 & 0 & 1.610 \end{bmatrix}, \quad [\beta^*] = \begin{bmatrix} 1.610 & 0 \\ 0 & 1.610 \end{bmatrix}, \quad [\kappa^*] = \begin{bmatrix} 1.638 & 0 \\ 0 & 1.638 \end{bmatrix}$$

This corresponds to the effective planar Lamé constants of $\lambda^* = \mu^* = 1.610$. As before, our solutions with $\beta^* = \lambda^* = \mu^*$ agree with the condition of $\alpha^* = \alpha_i = \alpha_m = 1/4$. Although these results show that the emerging effective properties lie between those of the constituent phases and the analytical bounds, the computed magnitudes do not follow conventional rules of mixtures.

Summary

We presented a physics-informed neural network-based first-order two-scale periodic asymptotic computational homogenization framework to determine the effective (macroscopic) thermoelastic properties of two-phase composites. The developed framework allowed the exact imposition of the periodic boundary conditions. Solving the relevant thermomechanical unit cell problems up to

a constant was sufficient to compute the integrals giving the effective properties. These allowed the training loss terms devoid of boundary condition contribution, eliminating the need for identifying the associated weights. We applied the developed framework to a planar composite with a circular inclusion of a hexagonal periodic unit cell. We showed that PINNs work successfully to solve emerging cell problems yielding the determination of effective thermomechanical properties.

References

[1] S. Torquato, Random Heterogeneous Materials, Microstructure and Macroscopic Properties, 1st ed. Interdisciplinary Applied Mathematics 16, Springer-Verlag New York, 2002.

[2] D. Lukkassen, L.-E. Persson, P. Wall, Some engineering and mathematical aspects on the homogenization method, Compos. Eng. 5 (1995) 519–531. https://doi.org/10.1016/0961-9526(95)00025-I

[3] C. Soyarslan, S. Batgmann, M. Pradas, J. Weissmuller, 3D stochastic bicontinuous microstructures: Generation, topology and elasticity, Acta Mater. 149 (2018) 326-340. https://doi.org/10.1016/j.actamat.2018.01.005

[4] C. Soyarslan, M. Pradas, S. Bargmann, Effective elastic properties of 3D stochastic bi-continuous composites, Mech. Mater. 137 (2019) 103098. https://doi.org/10.1016/j.mechmat.2019.103098

[5] C. Soyarslan, J. Havinga, L. Abelmann, T. van den Boogaard, Asymptotic homogenization in the determination of effective intrinsic magnetic properties of composites, Result. Phys. 44 (2023) 106188. https://doi.org/10.1016/j.rinp.2022.106188

[6] I. Lagaris, A. Likas, D. Fotiadis, Artificial neural networks for solving ordinary and partial differential equations, IEEE Transactions on Neural Networks 9 (1998) pp. 987-1000. https://doi.org/10.1109/72.712178

[7] G. Cybenko, Approximation by superpositions of a sigmoidal function, Mathematics of Control, Signals and Systems 2 (1989) 303–314. https://doi.org/10.1007/BF02551274

[8] K. Hornik, M. Stinchcombe, H. White, Multilayer feedforward networks are universal approximators, Neural Networks 2 (1989) 359–366. https://doi.org/10.1016/0893-6080(89)90020-8

[9] K. Hornik, M. Stinchcombe, H. White, Universal approximation of an unknown mapping and its derivatives using multilayer feedforward networks, Neural Networks 3 (1990) 551-560. https://doi.org/10.1016/0893-6080(90)90005-6

[10] L. Lu, X. Meng, Z. Mao, G.E. Karniadakis, DeepXDE: A Deep Learning Library for Solving Differential Equations, SIAM Review 63 (2021) 208–228. https://doi.org/10.1137/19M1274067

[11] I. Lagaris, A. Likas, D. Papageorgiou. Neural-network methods for boundary value problems with irregular boundaries, IEEE Transactions on Neural Networks 11 (2000) 1041-1049. https://doi.org/10.1109/72.870037

[12] J. Sirignano K. Spiliopoulos, DGM: A deep learning algorithm for solving partial differential equations, J. Computat. Phys. 375 (2018) 1339–1364. https://doi.org/10.1016/j.jcp.2018.08.029

[13] E. Haghighat, M. Raissi, A. Moure, H. Gomez, R. Juanes, A physics-informed deep learning framework for inversion and surrogate modeling in solid mechanics, Comp. Meth. Appl. Mech. Eng. 379 (2021) 113741.

[14] S. Cuomo, V. Schiano di Cola, F. Giampaolo, G. Rozza, M. Raissi, F. Piccialli, Scientific Machine Learning through Physics-Informed Neural Networks: Where we are and What's next, arXiv preprint (2022), arXiv: 2201.05624

[15] C. Soyarslan, M. Pradas, Physics-informed machine learning in asymptotic homogenization of elliptic equations. arXiv preprint (2023), arXiv: 2301.09725

[16] W. Nowacki, Dynamic Problems of Thermoelasticity, Polish Scientific Publishers Warszawa, Poland, 1975.

[17] R. Guinovart-Díaz, R. Rodriguez-Ramos, J. Bravo-Castilero, F.J. Sabina, G.A. Maugin, Closed-Form Thermoelastic Moduli of a Periodic Three-Phase Fiber-Reinforced Composite, J. Therm. Stress. 28 (2005) 1067–1093. https://doi.org/10.1080/014957390967730
[18] F.E. Neumann. Vorlesungen über mathematische Physik: Vorlesungen über die Theorie der Elasticität der festen Körper und des Lichtäthers. B. G. Teubner, Leipzig, 1885.
[19] J.F. Nye, Physical properties of crystals: their representation by tensors and matrices, Oxford University Press, 1985.